Increased Growth Synchrony of Red Spruce in Response to Acid Deposition Recovery and Climate Change across its Southern Range Extent, Southeastern USA

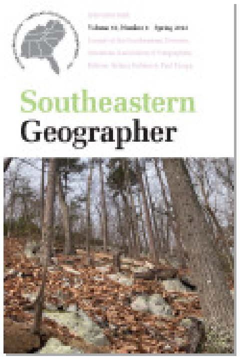

Maegen L. Rochner, Thomas W. Patterson, Karen J. Heeter, Grant L. Harley

Southeastern Geographer, Volume 63, Number 1, Spring 2023, pp. 78-97 (Article)

Published by The University of North Carolina Press
DOI: *https://doi.org/10.1353/sgo.2023.0006*

Increased Growth Synchrony of Red Spruce in Response to Acid Deposition Recovery and Climate Change across its Southern Range Extent, Southeastern USA

MAEGEN L. ROCHNER
University of Louisville

THOMAS W. PATTERSON
University of North Carolina at Chapel Hill

KAREN J. HEETER
Columbia Climate School, Lamont-Doherty Earth Observatory

GRANT L. HARLEY
University of Idaho

HIGHLIGHTS

- We present a new, spatially extensive red spruce tree-ring network from across southeastern US spruce refugia.
- High-elevation red spruce are largely unique and individualistic in growth patterns and climate response.
- Increased growth rates, growth synchrony, and climate response post-1990 indicate recovery following the CAAA.
- A region-wide shift towards synchrony and increased sensitivity highlights the potential for region-wide management strategies.
- Results provide a temporal perspective that can inform management under reduced air pollution and climate change.

ABSTRACT: *In a complex system of natural and human-caused disturbance, shifting climate, and documented, widespread decline and recovery of red spruce populations prior to and following the United States (US) Clean Air Act and amendments (CAAA) — all within the last century — a better understanding of the potential influence of these disturbances on the climate sensitivity and resiliency of red spruce under projected future conditions is needed. We investigated the potential recovery of annual growth in southeastern US red spruce populations following the CAAA and the influence of this recovery vs. ongoing climate change. Using a recently collected network of red spruce tree-ring data from across the southern Appalachian range, we examined temporal trends in stand-level growth and climate sensitivity in the context of acidic (acid) deposition and recovery and modern climate change.*

SOUTHEASTERN GEOGRAPHER, 63(1) 2023: pp. 78–97

We demonstrated that in recent decades, spruce growth is becoming synchronous and climate sensitive in conjunction with a reduction in acid deposition coupled with changes in climate conditions. The emergence of synchronous growth across sites is a new phenomenon that highlights the potential of and the need for region-wide management. Our results provide a temporal perspective that can aid future management strategies in an era of reduced air pollution and a changing climate.

KEYWORDS: Dendrochronology, Protected areas, Clean Air Act, Appalachia

INTRODUCTION

In temperate forests of the eastern United States (US), the red spruce (*Picea rubens* Sarg.) faces a complex combination of threats including air pollution and acidic deposition, insect outbreaks, and anthropogenically driven climate and land use change, prompting widespread concern for the future of the species (McLaughlin et al. 1987, White et al. 2014). These threats are even more pressing in the southeastern US, where the species naturally exists in disjunct populations across the southern Appalachian highlands (Figure 1). At its southernmost extent, red spruce, in combination with the endangered Fraser fir (*Abies fraseri* [Pursh] Poir.) comprise the isolated spruce-fir forest community, as climate refugia left over from the last glacial cycle (White and Cogbill 1992, Keppel et al. 2012, Heeter et al. 2019). In southern Appalachia, spruce-fir ecosystems possess unique ecological, economic, and recreational value and thus represent environmental legacies and heritage threatened by human-caused disturbances including climate change (Soulé 2011, White et al. 2014). Long-lived, high-elevation red spruce are also valuable sources of proxy climate information that are critical for contextualizing modern temperature change (Heeter et al. 2019). Future conservation and management of red spruce and spruce-fir ecosystems in the southern Appalachian region, including those on state, federal, and privately protected lands, therefore require a better understanding of the potential influence of these disturbances on the climate sensitivity and resiliency of red spruce under projected future conditions.

Widespread declines of spruce forests following the mid-1960s are attributed to increased rates of acidic deposition prior to the US Clean Air Act and Amendments (CAAA) in 1970 and 1990 (Greaver et al. 2012). The “last stand of the red spruce” (Mello 1987) prompted intense study through the 1990s and early 2000s, as extended impacts of acidic deposition on growth were documented as late as 2003 (Adams and Eagar 1992, Cook and Zedaker 1992, Lazarus et al. 2004). Red spruce decline has been attributed to acidic deposition-induced nutrient disruption, such as the loss of calcium, which leads to leaf defoliation and susceptibility to further ecosystem degradation (DeHayes et al. 1999, Schaberg et al. 2000, Driscoll et al. 2001). However, later studies assessing radial growth patterns discovered that red spruce had recovered in the more continuous areas of the species range in the US northeast and into the central Appalachian highlands (Kosiba et al. 2013, 2017, 2018, Engel et al. 2016, Wason and Dovciak 2017, Mathias and Thomas 2018, Yetter et al. 2021). To date, relatively few studies have examined growth recovery for the southern Appalachian highlands, although the limited research

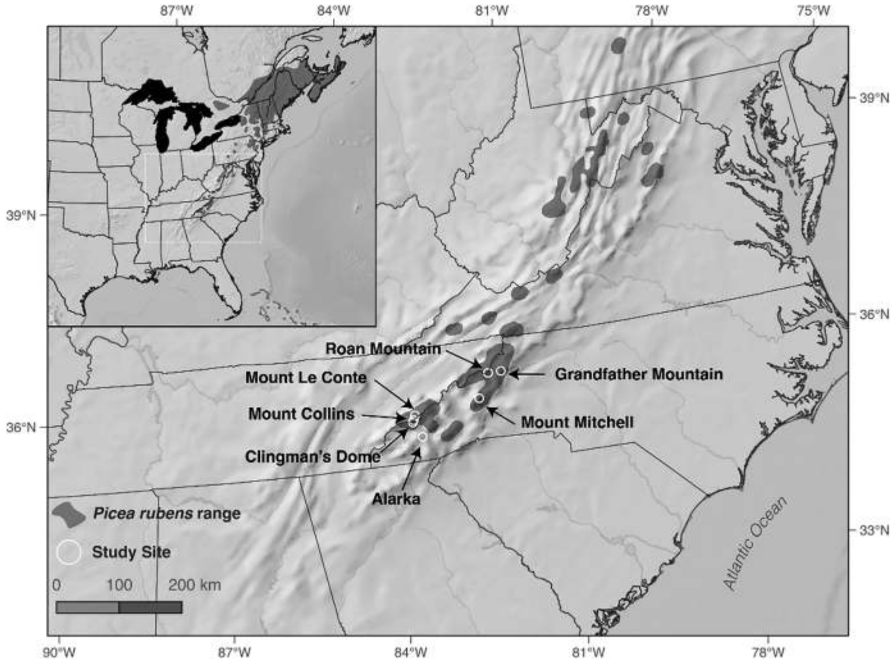

Figure 1. Southeast US P. rubens *tree-ring network. Map showing names and locations of the seven tree-ring study sites at the southern geographic range extent for* P. rubens *along the southern Appalachian Mountains.*

indicates growth decline may not have been as universal across the southern extent of the species' range (Cook and Zedaker 1992, Schuler and Collins 2002, Koo et al. 2011, Soulé 2011, White et al. 2014).

Compared to the core distribution of red spruce in the US northeast and Canada, the disjunct populations of southern Appalachia remain understudied and potentially unique from northeastern populations. In a complex system of natural and human-caused disturbance, shifting climate, and documented, widespread decline and recovery of red spruce populations prior to and following the US CAAA — all within the last century — a better understanding of the potential influence of these disturbances on the climate sensitivity and resiliency of red spruce under projected future conditions is needed. The objective of this work is to use tree-ring methods to investigate potential recovery in the growth of southeastern red spruce populations following the CAAA and the influence of this recovery vs. ongoing climate change on climate sensitivity. Using a recently collected network of red spruce tree-ring data from across the southern Appalachian range, we examined temporal trends in stand-level growth and climate sensitivity in the context of acidic deposition and recovery and modern climate change. A broader spatial analysis of red spruce populations will highlight if regional conservation strategies may be possible, or if the complex differences highlighted by previous studies from southern

Appalachia (Cook and Zedaker 1992, Schuler and Collins 2002, Koo et al. 2011, Soulé 2011, White et al. 2014) will continue to present challenges to the protection of spruce-fir ecosystems under climate change, despite ecosystem recovery from acid deposition.

METHODS

Study Sites and Tree-Ring Datasets

A new, spatially extensive, high-elevation network of red spruce tree-ring data from across the southeastern US (Heeter et al. 2019, Harley et al. 2021) presented an opportunity for tree-ring analyses of spruce recovery in southeastern Appalachia. This network includes seven montane sites from the region (Table 1, Figure 1). Trees sampled were mostly located on ridge tops and north-facing slopes at high elevations (> 1800 m), with the exception of Alarka, which is located in a lower elevation (1260 m), cold-air bog. Alarka represents the southernmost identified population of red spruce in eastern North America (Collins et al. 2010). All seven sites are located within a protected area, including state parks and national parks and forests (Table 1). Acid deposition data for three collection sites (National Atmospheric Deposition Program [NADP]) from southern Appalachia indicate improving conditions post-1990 (Figure 2A, B). However, historical context for this improvement, i.e., conditions during the height of spruce decline, are not available, limiting analyses of relationships between spruce growth and acid conditions prior to and following the CAAA. Concurrent with acid deposition recovery, on average all seven sites experienced cooler and wetter conditions after 1990 (Figure 2C–H).

We collected tree-ring samples using an increment borer and mounted, sanded, and processed all samples according to standard dendrochronological techniques (Speer 2010). We measured tree-ring widths using high-resolution scanned images and the software CooRecorder (Larsson 2014) and confirmed the dating accuracy of tree rings using time series correlation analyses in the software COFECHA (Holmes 1983). To standardize raw ring widths, we used a two-thirds smoothing spline and bi-weight robust mean estimation in the R dendrochronology program library (dplR) (Mosteller and Tukey 1977, Cook 1985, Bunn 2008) and developed final tree-ring chronologies for each of the seven sites (Table 2).

Site Comparisons and Temporal Trends in Growth

We first compared the chronologies across sites for similarities and differences in growth patterns over the common period (1889–2008 CE) using Pearson's r correlations and principal component analysis (PCA). We also examined broader spatial synchrony in growth patterns by calculating moving (30-year moving window) cross-correlations (Pearson's r) between pairs of sites from 1895 to the year of most recent growth. We examined the chronologies for statistical shifts in mean annual growth using regime shift detection software version SRDS 6.2.1 (Rodionov 2004). We maintained regime shift program defaults across all analyses (target significance = 0.05, 20-year cut-off length, Huber's tuning constant = 2). Individual site histories were unknown and could influence the magnitude of each regime shift; therefore, we did not make comparisons in the size of each regime shift but rather we recorded each shift as present/absent.

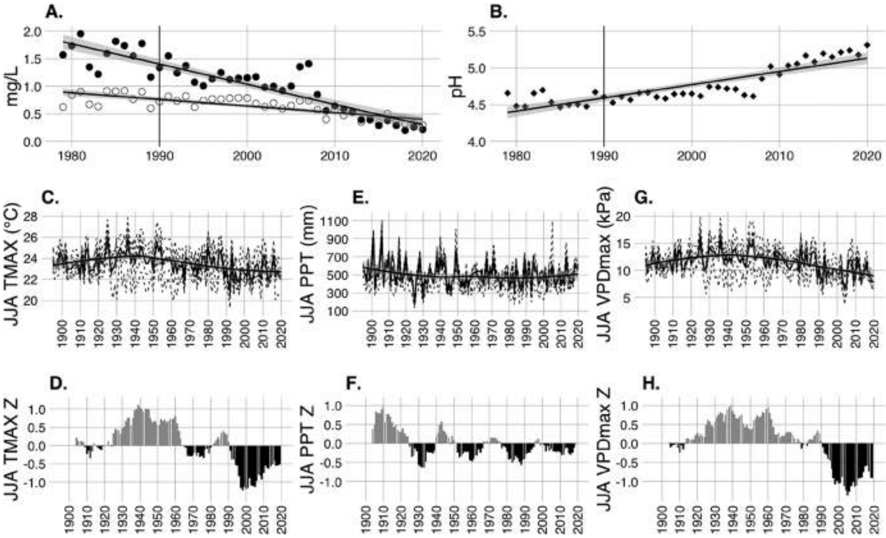

Figure 2. Average acid and climate conditions across the P. rubens *network. (A.) Average annual wet deposition concentration of nitrates (unshaded) and sulfates (shaded) and (B.) soil acidity (pH) for three atmospheric stations combined (Mount Mitchell, Great Smoky Mountains National Park, Coweeta Research Lab), 1979–2020, downloaded from https://nadp.slh.wisc.edu/maps-data/ntn-interactive-map/. (C–H.) Instrumental climate data, PRISM 4x4 km grid cell for each study site (dashed lines) and the average for all sites (black line and loess smoother) with calculated average z-scores (10-year running average) for combined June, July, and August (JJA) (C–D.) TMAX, (E–F.) PPT, and (G–H.) VPDmax.*

Table 1. Site attributes of the southeast US P. rubens *tree-ring network.*

Site	Site Code	State	Elevation (m)	Latitude/Longitude	Site Management
Alarka	ACS	NC	1260	35.34, -83.35	Nantahala National Forest
Clingman's Dome	CDS	TN/NC	2022	35.56, -83.49	Great Smoky Mountains National Park
Grandfather Mountain	GFM	NC	1812	36.11, -81.81	Grandfather Mountain Stewardship Foundation and State Park
Mount Collins	MCS	TN/NC	1883	35.59, -83.47	Great Smoky Mountains National Park
Mount Le Conte	MLC	TN	2010	35.65, -83.43	Great Smoky Mountains National Park
Mount Mitchell	MMS	NC	1976	35.77, -82.26	Mount Mitchell State Park
Roan Mountain	RMS	TN/NC	1916	36.11, -82.04	Roan Mountain State Park

Table 2. Chronology statistics for the southeast US P. rubens *tree-ring network***.** *The EPS, or expressed population signal, is a calculation of the representative power, or common signal, in the chronology, based primarily on sample depth and interseries correlation (Wigley et al. 1987).*

Site	# series	# trees	Years	Interseries Correlation	Mean Sensitivity	EPS	EPS Cutoff Year (< 0.80)
ACS	30	18	1889–2018	0.46	0.20	0.88	1944
CDS	21	12	1788–2018	0.48	0.23	0.81	1894
GFM	45	24	1826–2020	0.50	0.22	0.91	1871
MCS	25	14	1681–2018	0.57	0.21	0.83	1844
MLC	52	30	1767–2014	0.50	0.21	0.91	1864
MMS	26	16	1819–2018	0.43	0.24	0.78	1944
RMS	80	71	1874–2008	0.54	0.23	0.91	1934

Climate-Growth Response and Temporal Stability

To investigate the climate-growth relationships of red spruce and temporal stability of these relationships over the instrumental period, we used static and moving correlation analyses in the R package treeclim (Zang and Biondi 2015). We evaluated relationships between tree growth and monthly average temperature (TMEAN), monthly average maximum temperature (TMAX), monthly average minimum temperature (TMIN), total monthly precipitation (PPT), and monthly average maximum vapor pressure deficit (VPDmax) downloaded for each site from the 4x4 km resolution Partial Regression on Independent Slopes Model dataset (PRISM 2022). We considered climate-growth relationships to be temporally stable when they remained consistently positive or negative and statistically significant over the instrumental period or common period of overlap between the instrumental climate data and chronologies. Analyses of temporal stability allowed for investigation of potential correspondence between environmental changes, especially the CAAA, and nonstationarity of climate sensitivity, or the fading or shifting of climate-growth response over time.

RESULTS

Site Comparisons and Analyses of Growth

All chronologies are correlated with one another during the common period of analysis from 1889 to 2008, and similar growth patterns can be seen across the seven sites (Figure 3A, B). The strength of site-to-site correlations is not strong and only one pairing (CDS and MLC) exceeds $r > 0.50$ ($p < 0.001$). That said, nine pairings have modest, positive correlations of $r > 0.40$ (four pairs, $p < 0.001$) and $r > 0.30$ (five pairs, $p < 0.001$) (Figure 3E), which are not outside the typical range for regional tree-ring networks from the eastern US (e.g., Speer et al. 2009, George 2014, Copenheaver et al. 2020). While the highest correlated pair (CDS and MLC) are geographically clustered,

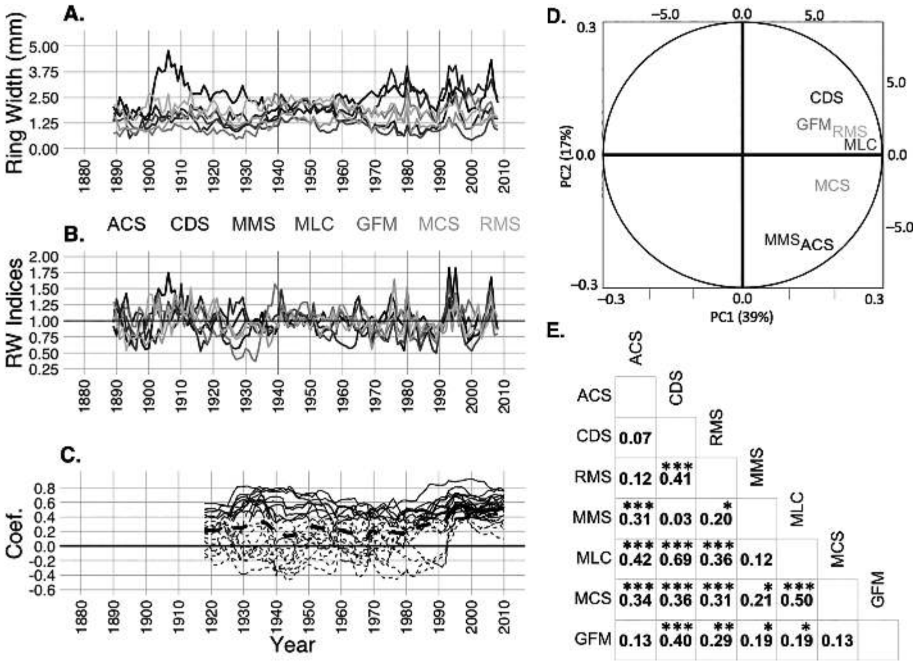

	ACS	CDS	RMS	MMS	MLC	MCS	GFM
ACS							
CDS	0.07						
RMS	0.12	*** 0.41					
MMS	*** 0.31	0.03	* 0.20				
MLC	*** 0.42	*** 0.69	*** 0.36	0.12			
MCS	*** 0.34	*** 0.36	*** 0.31	* 0.21	*** 0.50		
GFM	0.13	*** 0.40	** 0.29	* 0.19	* 0.19	0.13	

Figure 3. Site comparisons and growth synchrony. (A.) Average raw ring-width chronologies for all seven sites, (B.) Standardized index chronologies for all seven sites, (C.) Moving 30-year correlations (Pearson's r*) between all chronology pairings (n = 21) starting in 1895 through the year of final growth. Date on the x-axis indicates the final year of the 30-year window. The lines are solid when the 30-year correlation is significant (*$p < 0.05$*) and positive and dashed when not statistically significant (*$p > 0.05$*). The bold black line is the average value of all pairings. (D.) Results from PCA, and (E.) Correlation matrix for all 21 site pairings over the period 1889–2008,* $p < 0.001$****,* $p < 0.01$***,* $p < 0.05$**.*

this pattern did not persist for all correlated pairs, indicating common signals, although weak, in the seven chronologies across the broader geographic range of the study sites. A lack of geographic clustering in common signals is also indicated by PCA, as sites are not clustered in ordination space according to spatial proximity (Figure 1, 3D). Sites also are not clustered by elevation, e.g., MMS (1976 m) and ACS (1260 m). The chronologies for sites ACS and MMS contain a higher number of younger trees and both have an expressed population signal (EPS) — a metric that measures the shared, common signal amongst records — cutoff of 1944. The chronology for site RMS also contains a higher number of young trees but also the highest sample size of the seven chronologies, perhaps explaining its separation from ACS and MMS in the PCA.

Growth synchrony between the seven site chronologies increased after 1990 (Figure 3C). Moving correlation analyses of all possible pairings ($n = 21$) revealed that only 39 percent of the chronologies experience positive correlations for all of the 30-year windows prior to 1990; however, this percentage nearly doubles to 78 percent for

Table 3. Pre- and post-1990 correlations for site pairings, $p < 0.001$****,* $p < 0.01$***,* $p < 0.05$**.*

Pairing	Pre-1990 (1889–1989)	1990–2008
ACS-CDS	-0.08	0.48*
ACS-RMS	0.09	0.22
ACS-MMS	0.28**	0.52*
ACS-MLC	0.24*	0.88***
ACS-MCS	0.25*	0.81***
ACS-GFM	0.15	-0.03
CDS-RMS	0.36***	0.61**
CDS-MMS	-0.15	0.80***
CDS-MLC	0.66***	0.76***
CDS-MCS	0.31**	0.62**
CDS-GFM	0.45***	0.22
RMS-MMS	0.14	0.58**
RMS-MLC	0.37***	0.39
RMS-MCS	0.30**	0.40
RMS-GFM	0.30**	0.20
MMS-MLC	-0.01	0.63**
MMS-MCS	0.17	0.62**
MMS-GFM	0.13	0.55*
MLC-MCS	0.44***	0.77***
MLC-GFM	0.26**	-0.08
MCS-GFM	0.14	0.12

all windows that include dates post-1990. A comparison of pre- and post-1990 correlations (Pearson's *r*) also displays improvement in correlations between pairings (Table 3), except for in pairs that include GFM, which in some cases show decreasing synchrony, perhaps due to changes unique to GFM post-1990. Overall, these findings indicate that only modest agreement among the chronologies persisted prior to the CAAA, and afterward spatial agreement across the network has greatly improved.

All chronologies contain regime shifts in mean annual growth (Figure 4A). Prior to *ca.* 1940, all chronologies experienced two regime shifts in growth, yet the direction of the shifts was inconsistent. The only congruent pattern early in the time series is a collective regime shift for six out of the seven chronologies to narrower ring width during the period of 1913–1924. After this early period of volatility, each chronology experienced one to two regime shifts in mean growth, but the direction and time of shift were inconsistent. That said, a collective shift to prolonged, reduced growth occurred *ca.* 1960–1990 before returning to normal post-CAAA. Considering lower-frequency changes to mean annual growth, we examined average growth across all seven sites for five-year increments (hereafter "pentads") and found results that reflected the regime shifts (Figure 4B). The growth decline of the late 1910s–early 1920s persisted through the 1940s when some of the lowest growth was recorded. Average growth stabilized until *ca.* 1960 when a second decline occurred that persisted until the 1990–1995 pentad. During the

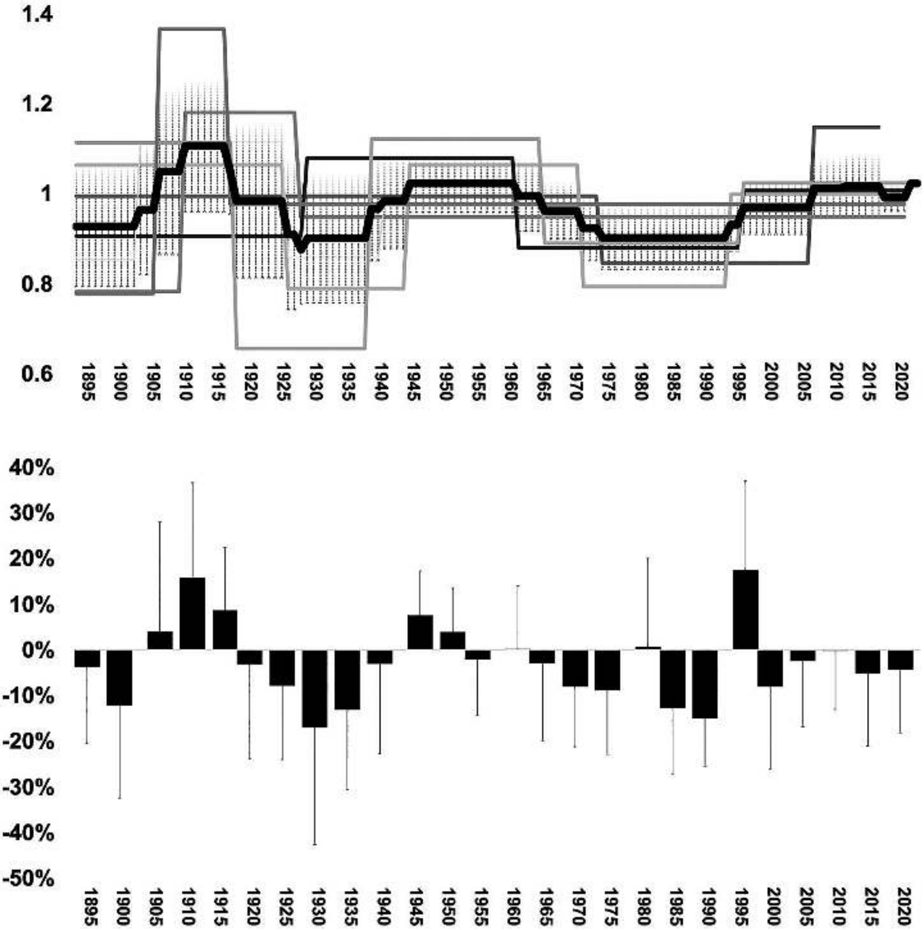

Figure 4. Temporal trends in growth. (A.) Regime shifts in mean growth for the seven spruce chronologies (thin lines) with the overall average value of all seven sites (bold line with standard-error stippling). (B.) Pentad growth changes for mean annual growth averaged across all seven sites (with standard deviation bars). Year on the x-axis signifies the final year of the 5-year pentad.

five years following the CAAA, average growth across the seven sites increased by 17.5 percent (SD 19.0 percent) and produced the largest pentad growth change across the common period. After this pentad growth surge, average growth in all remaining pentads became slightly negative, indicating a long-term decline since *ca.* 1960 that was punctuated with one large growth release in the five years following the CAAA.

Climate-Growth Response

Static relationships (Pearson's *r*) between ring-width indices (RWI) and monthly temperature variables are not consistent across the seven study sites. While all but one

Table 4. Static correlations between ring-width indices and monthly temperature variables, previous and current May–September and February. Significant relationships ($p < 0.05$) are indicated by bold font. Only those months with at least one statistically significant relationship with at least one temperature variable are shown.

(A) Average Monthly Temperature (TMEAN)

Site	pMay	pJun	pJul	pAug	pSep	Feb	May	Jun	Aug	Sep
ACS	-0.12	**-0.20**	-0.07	**-0.21**	0.00	**-0.17**	**-0.19**	**-0.20**	-0.03	0.03
CDS	0.09	-0.03	-0.06	-0.17	-0.19	-0.07	0.09	-0.04	0.01	-0.16
GFM	0.10	-0.03	-0.05	0.02	-0.16	-0.14	-0.03	-0.03	0.09	-0.16
MCS	-0.04	-0.14	**-0.17**	-0.16	-0.08	-0.05	-0.14	-0.10	0.07	-0.02
MLC	-0.17	-0.02	-0.09	-0.11	-0.02	0.03	-0.16	-0.01	0.02	0.16
MMS	-0.10	0.00	-0.06	-0.09	0.00	0.02	-0.16	-0.07	-0.06	0.15
RMS	0.12	0.06	-0.05	-0.08	**-0.25**	-0.09	0.08	0.09	0.18	0.02

(B) Average Monthly Maximum Temperature (TMAX)

Site	pMay	pJun	pJul	pAug	pSep	Feb	May	Jun	Aug	Sep
ACS	**-0.19**	**-0.29**	-0.10	**-0.28**	-0.08	-0.16	**-0.23**	**-0.19**	-0.08	-0.02
CDS	0.08	-0.08	-0.13	-0.22	-0.14	-0.06	0.13	-0.03	-0.04	-0.13
GFM	0.12	-0.04	-0.16	-0.02	-0.09	-0.16	0.04	-0.02	0.08	-0.07
MCS	-0.06	-0.15	**-0.17**	-0.15	-0.08	0.00	-0.10	-0.02	0.10	0.00
MLC	-0.17	-0.08	-0.15	-0.16	-0.03	0.01	-0.17	-0.05	0.00	0.14
MMS	-0.08	-0.06	-0.06	-0.09	-0.05	0.04	-0.14	-0.09	-0.04	0.06
RMS	0.11	0.00	-0.11	-0.08	**-0.21**	-0.10	0.12	0.07	0.11	-0.04

(C) Average Monthly Minimum Temperature (TMIN)

Site	pMay	pJun	pJul	pAug	pSep	Feb	May	Jun	Aug	Sep
ACS	-0.03	-0.05	-0.01	-0.05	0.07	**-0.17**	-0.12	**-0.17**	0.04	0.07
CDS	0.09	0.04	0.05	-0.04	**-0.19**	-0.07	0.05	-0.04	0.07	-0.16
GFM	0.07	-0.03	0.08	0.06	**-0.20**	-0.12	-0.08	-0.05	0.08	**-0.23**
MCS	-0.02	-0.12	-0.12	-0.11	-0.07	-0.10	-0.15	-0.16	0.02	-0.04
MLC	-0.13	0.06	0.00	-0.02	0.00	0.05	-0.12	0.04	0.04	0.16
MMS	-0.13	0.05	-0.04	-0.06	0.07	0.00	-0.15	-0.03	-0.05	**0.19**
RMS	0.10	0.12	0.04	-0.04	**-0.23**	-0.08	0.01	0.09	**0.18**	0.10

Table 5. Static correlations between ring-width indices and monthly moisture variables. Significant relationships ($p < 0.05$*) are indicated by bold font. Only those months with at least one statistically significant relationship with either PPT or VPDmax are shown.*

(A) Precipitation (PPT)

Site	pMay	pJun	pJul	pAug	pSep	pOct	pNov	pDec	April	May	Jul
ACS	0.13	**0.21**	0.18	**0.25**	0.10	-0.06	**0.18**	0.05	-0.03	0.00	0.06
CDS	**-0.21**	0.11	0.10	**0.25**	-0.03	-0.06	-0.05	0.00	**-0.18**	**-0.24**	-0.04
GFM	**-0.22**	0.10	0.10	0.07	0.00	**-0.21**	-0.01	-0.18	-0.02	**-0.22**	-0.01
MCS	0.08	0.06	0.11	0.10	0.12	-0.01	0.10	0.02	-0.13	0.08	-0.05
MLC	0.08	-0.04	-0.06	0.10	0.03	**-0.16**	0.04	0.02	-0.03	0.08	-0.13
MMS	0.06	0.03	0.03	0.17	0.06	-0.08	0.07	0.02	-0.15	-0.01	-0.12
RMS	-0.01	0.16	-0.05	0.00	0.04	-0.08	-0.13	0.03	-0.05	-0.17	**-0.23**

(B) Maximum Vapor Pressure Deficit (VPDmax)

Site	pMay	pJun	pJul	pAug	pSep	pOct	pNov	pDec	April	May	Jul
ACS	**-0.35**	**-0.34**	-0.16	**-0.35**	-0.15	-0.16	-0.06	0.00	0.10	-0.12	0.00
CDS	0.00	-0.14	**-0.18**	**-0.20**	-0.05	0.08	**0.20**	**-0.18**	-0.07	0.14	0.05
GFM	0.09	-0.09	**-0.21**	-0.07	-0.01	0.06	0.13	-0.12	0.07	0.10	-0.10
MCS	-0.12	-0.14	**-0.18**	-0.14	-0.07	0.07	**0.25**	-0.01	**0.22**	-0.06	0.08
MLC	**-0.19**	-0.16	**-0.18**	**-0.22**	-0.10	0.04	0.06	0.09	0.06	-0.19	0.04
MMS	-0.05	-0.14	-0.10	-0.14	**-0.13**	-0.01	0.10	0.07	0.14	-0.10	0.02
RMS	0.04	-0.04	-0.03	-0.04	-0.06	0.12	0.10	-0.10	-0.08	**0.22**	**0.19**

of the sites (MLC) display at least one significant ($p < 0.05$) relationship between RWI and TMEAN, TMAX, or TMIN, growth responses are rarely consistent across months, and significant correlations do not exceed +/- 0.29 (Table 4). Relationships with temperature variables are consistently negative, except for between RWI and current August and September TMIN for MMS and RMS. Some sites show an inverse response to temperature variables. For example, RWI at GFM is negatively correlated with current September TMIN, while RWI at MMS is positively correlated with the same variable. In addition to this example of an opposing response, the only other monthly variable that is significantly correlated with RWI at more than one site is previous September TMIN (Table 4). The lowest elevation site, ACS, displays the most significant relationships — all negative — between RWI and temperature variables.

Static relationships between RWI and monthly PPT and VPDmax variables are more consistent than for temperature across the seven study sites. All seven sites display at least one significant relationship with either PPT or VPDmax with some consistency across months (Table 5). However, correlations are again low, no greater than +/- 0.35, and

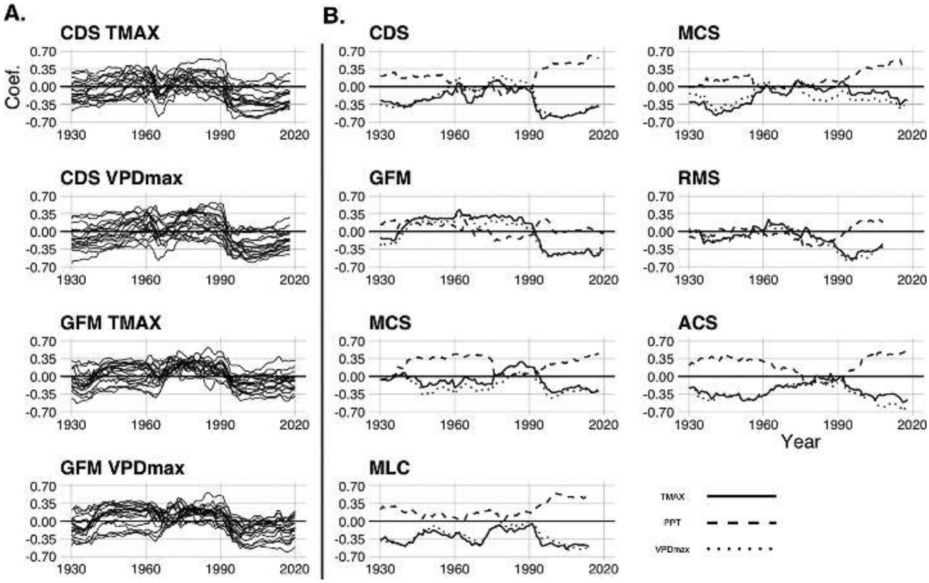

Figure 5. Moving climate-growth responses. (A.) Examples of shifting, fading responses to climate from CDS and GFM: Moving correlations, 35-year windows, between ring-width indices and monthly climate variables (all months previous May to current October). (B.) Moving correlations between ring-width indices and previous August TMAX (solid line), PPT (dashed line), and VPDmax (dotted line).

no relationship is consistent across all sites. Overall, previous-year PPT and VPDmax are more dominant drivers of growth than current year conditions. VPDmax during the previous year growing season, May, June, July, or August, in particular is the most consistent response across sites. Like with temperature, ACS displays the greatest number of significant correlations and strongest relationships with monthly PPT and VPDmax variables.

Temporal Stability of Climate-Growth Response

Across all seven sites, moving relationships (Pearson's *r*) between RWI and monthly temperature, PPT, and VPDmax variables are not temporally stable over the instrumental period. All sites experienced some fading, shifting, or emerging responses over time. Even relationships that were consistently positive or negative experienced some weakening to near zero for some portion of the instrumental period (Figure 5A). These nonstationarities in climate-growth response likely account for the overall low static correlations between RWI and monthly climate variables calculated over the common period (Table 4, 5). A common pattern across most of the sites, and particularly CDS and GFM, is a weakening or shifting of climate relationships between the 1960s/70s and 1990s, with the emergence or re-emergence of strong responses to previous-year growing season conditions post-1990 (Figure 5A). For example, across all sites, relationships with previous August TMAX, PPT, and VPDmax, the most consistent emerging response across all seven sites strengthened post-1990 after weakening to near zero at some point between the 1960s and 1990s (Figure 5B). This shift indicates increasing sensitivity to previous summer moisture stress (i.e., positive relationships with PPT and negative relationships with TMAX and VPDmax) after 1990, consistent across all seven study sites.

DISCUSSION

We found that high-elevation red spruce, even in geographic proximity to the southern range limit, are largely individualistic in growth patterns and climate response, a finding that aligns with other similar studies of species networks in forests of eastern North America, including boreal (e.g., Nicault et al. 2015, Ashiq and Anand 2016) and lower-elevation mesic forests (Zhang et al. 2015, Copenheaver et al. 2020). In this study, we identified only weak common signals across the seven study sites (although $> r = 0.30$), and ring widths did not display strong or consistent static relationships with any climate variable. Further, we found climate-growth relationships to be temporally unstable. Despite the selection of trees from high-elevation climate refugia, neither temperature nor moisture conditions appear to be the dominant drivers of radial growth across the network over the full instrumental period. Poor synchrony in growth, and particularly in climate response, is not unusual in red spruce. Multiple studies have identified temporal instability in climate-growth response of the species, often occurring during the middle of the 20th century and attributed to climate change and high rates of disturbance, including balsam wooly adelgid infestations and acid deposition (Cook 1987, Johnson et al. 1988, Cook and Johnson 1989, White 2010, Soulé 2011, White et al. 2014).

Across the red spruce network analyzed for this study, tree growth over the last century has largely been driven by non-climate factors, including acid deposition, as evidenced by weakened growth response at all sites between the 1960s and 1990s (Figure 5). Other potential factors contributing to individualistic responses include site-specific high rates of disturbance, histories of logging, and competition (Fraver et al. 2009). Potentially, increased synchrony post-1990 corresponds alternatively with reductions in competition following canopy recruitment, although this would require synchronous canopy recruitment across the entire network. Such complexities require the addition of plot-level demographic data. Differences in the timing of shifts and/or weakening in climate response across sites is potentially related to local variations in the timing (including duration) and magnitude (amount) of acid deposition, differences in soil buffering capacities across space, and localized influences of acid deposition on climate vulnerability, particularly to cold (Kosiba et al. 2018), and isolated weather events, influenced by the highly variable Appalachian terrain, such that sites can experience unique conditions despite broader, regional weather patterns (Perry and Konrad 2006, Prat and Barros 2010).

Despite overall weak correspondence and individualistic climate responses over much of the instrumental period, we found increased growth rates, growth synchrony, and climate response across the network post-1990, indicating acid deposition recovery following the CAAA. Prior to 1990, and for all sites between the 1960s and 1990s, low growth synchrony and climate sensitivity can likely be attributed to masking by the influence of acid deposition, the influence of which would have varied in timing and magnitude between sites. The same period corresponds with a period of relatively average climate, highlighting the dominant influence of acid deposition but also the potential role of climate stability and a lack of extreme variability in decreased growth sensitivity over the same period. The 1960s–1990s is a period of stabilization after the Dust Bowl of the 1930s–40s in North America (Stahle et al. 2007), which coincides with higher TMAX, VPDmax (Figure 2D, H), and reduced growth (Figure 4) across sites, and increased moisture sensitivity at some sites (Figure 5B). After 1990, acid recovery across the sites is also potentially compounded by climate influences, as shifts in both temperature and VPD max, towards cooler and more humid conditions, also occur after 1990 and may have benefitted growth (Figure 2C–H). Increased rates of growth correspond with increased sensitivity to previous summer conditions affecting moisture stress (i.e., positive relationships with PPT and negative relationships with TMAX and VPDmax) (Figure 5). Unlike during the Dust Bowl, this response is likely due to positive growth during cooler, more humid conditions rather than negative responses to increased moisture stress: the potential combined influence of CAAA benefits and a cooler, more humid climate.

Site-specific, individualistic growth patterns and sensitivity to climate and acid deposition complicate or even negate region-wide management strategies and predictions of future response to climate. However, a region-wide shift towards synchrony and increased sensitivity to previous-year moisture stress indicates potential for broader-scale management of red spruce in southern Appalachia. In particular, increased sensitivity to previous summer moisture stress would affect how red spruce should be managed under projected future climate conditions. While cooler and more humid conditions potentially benefitted red spruce growth during acid deposition recovery, a warming and drying trend from the 2000s to present (Figure 2C–H) may lead to increased climate stress. Persistent cooler, wetter conditions in southern Appalachia after the Dust Bowl highlight the role of the Appalachian Mountains as potential refugia from modern climate change, but projected future changes predict overall warmer, drier conditions in the southern portion of the range (Fernandez and Zegre 2019).

The most recent literature concerning growth changes in red spruce show a mixed response of mean growth changes that are often attributable to climatic relationships. For example, Kosiba et al. (2018) found a positive-growth change across the northeastern US that they attribute to warmer average temperatures outside of the traditional growing season coupled with reductions in acid deposition. Similarly, and farther south in the species' range, Mathias and Thomas (2018) showed an improvement in central Appalachian red spruce growth post-CAAA that they attribute to reductions in acid deposition and increased CO_2 but not temperature. These two studies indicate a positive trend in growth for the near future assuming current environmental conditions persist. That said, the future climate projections that predict warmer temperatures may lead to reduced growth for red spruce in the southern portion of the species' range. Studies conducted within red spruce stands in West Virginia (Yetter et al. 2021) and Great Smoky

Mountains National Park (Koo et al. 2011) show a detrimental effect of increased temperatures on growth that may not be offset by the growth benefit of reduced air pollution. Our results differed from these previous studies in that we analyzed a moving-climate relationship and found that climate did not significantly influence growth at the seven sites until the CAAA. Conversely, our results confirm the growing consensus that climate will have an important influence on growth in the near future as indicated by the recent emergence of climate sensitivity across all sites and the networked synchrony of growth post-CAAA.

The collection of a new, spatially extensive network of red spruce chronologies from across southeastern spruce refugia presented an opportunity to analyze spruce growth and climate response in the context of the CAAA and climate change in southern Appalachia. While this work presents only a surface-level and tree-ring-focused analysis, it highlights increased future potential for network-scale analyses. Across the southern spruce populations analyzed for this study, we interpret the increased synchrony among sites since the 1990s as new opportunities to examine red spruce across a broader range, such as through the formation of a red spruce network or consortium, that could be partnered with restoration groups such as the Southern Appalachian Spruce Restoration Initiative (SASRI 2022). This consortium could focus on the collection of additional red spruce tree-ring data, highlighted by this study to be important for assessment of growth synchrony and climate sensitivity, but should also focus on other tree-ring metrics that may perform better as proxies for climate reconstruction. We found that tree-ring widths were not significantly driven by climate variability and that climate-growth responses were inconsistent across sites pre-1990 CAAA. Other tree-ring metrics, such as blue intensity, may be more consistently and significantly responsive to climate than total ring width (Heeter et al. 2019). However, we do not discount the need for increased plot-level demographic and ecological data to assist in the disentangling of climate and anthropogenic impacts like pollution from ecological factors such as species differences, competition, canopy structure, and disturbance, which would better inform the complexities highlighted by this study. Long-term, range-wide studies of red spruce that combine climate, ecology, and human-environment interactions are necessary to better predict the future of red spruce under ongoing environmental change.

CONCLUSIONS

At present, over 90 percent of spruce-fir ecosystems are managed under national or state parks and forests (USFS 2022), and this network of management provides a unique opportunity to consider strategies that can be implemented at a range-wide scale. We have demonstrated in our findings that spruce growth is becoming synchronous and climate sensitive due to what we interpret as a reduction in acid deposition coupled with changes in climate conditions in the most recent decades. Regardless of the drivers of change, the emergence of synchronous growth across sites is a new phenomenon that provides a line of evidence toward the need for region-wide management. Our results provide a temporal perspective that can aid future management strategies in an era of reduced air pollution and a changing climate.

ACKNOWLEDGEMENTS

We thank the following: Dr. Justin Maxwell, Dr. Stockton Maxwell, Dr. Joshua Bregy, Danny King, Laura Smith, Tsun Fung Au, and Ben Lockwood for field assistance, Dr. Saskia van de Gevel and Philip White for donation of Roan Mountain tree-ring data, and Gary Wein at the Highlands-Cashiers Land Trust for assistance with logistics at the Alarka site. This research was funded by the US National Science Foundation Paleo Perspectives on Climate Change program (P2C2; AGS-1805276 and AGS-2002524).

REFERENCES CITED

Adams, M.B., and Eagar, C. 1992. Impacts of Acidic Deposition on High-Elevation Spruce-Fir Forests: Results from the Spruce-Fir Research Cooperative. *Forest Ecology and Management* 51 (1-3): 195–205. https://doi.org/10.1016/0378-1127(92)90485-R.

Ashiq, M.W., and Anand, M. 2016. Spatial and Temporal Variability in Dendroclimatic Growth Response of Red Pine (*Pinus resinosa* Ait.) to Climate in Northern Ontario, Canada. *Forest Ecology and Management* 372: 109–19. https://doi.org/10.1016/j.foreco.2016.04.008.

Bunn, A.G. 2008. A Dendrochronology Program Library in R (dplR). *Dendrochronologia* 26 (2): 115–24. https://doi.org/10.1016/j.dendro.2008.01.002.

Collins, B, Schuler, T.M., Ford, W.M., and Hawkins, D. 2010. Stand Dynamics of Relict Red Spruce in the Alarka Creek Headwaters, North Carolina. In *Proceedings from the Conference on the Ecology and Management of High-Elevation Forests in the Central and Southern Appalachian Mountains,* edited by J. Rentch and T.M. Schuler. 22–27. U.S. Department of Agriculture, Forest Service.

Cook, E.R. 1985. A time series analysis approach to tree-ring standardization. Ph.D. dissertation. University of Arizona, Tucson.

Cook, E.R. 1987. The Use and Limitations of Dendrochronology in Studying Effects of Air Pollution on Forests. In *Effects of Atmospheric Pollutants on Forests, Wetlands and Agricultural Ecosystems*, edited by T.C. Hutchinson and K.M. Meema. Springer. https://doi.org/10.1007/978-3-642-70874-9_20.

Cook, E.R. and Johnson, A.H. 1989. Climate Change and Forest Decline: A Review of the Red Spruce Case. *Water, Air, and Soil Pollution* 48(1): 127–40. https://doi.org/10.1007/BF00282374.

Cook, E.R., and Zedaker, S.M. 1992. The Dendroecology of Red Spruce Decline. In *Ecology and Decline of Red Spruce in the Eastern United States,* edited by C. Eager and M. Adams. 192–231. Springer. https://doi.org/10.1007/978-1-4612-2906-3_5.

Copenheaver, C.A. et al. 2020. Dendroclimatology of Sugar Maple (*Acer saccharum*): Climate-Growth Response in a Late-Successional Species. *Dendrochronologia* 63: 125747. https://doi.org/10.1016/j.dendro.2020.125747.

DeHayes, D.H., Schaberg, P.G., Hawley, G.J., and Strimbeck, G.R. 1999. Acid Rain Impacts on Calcium Nutrition and Forest Health: Alteration of Membrane-Associated Calcium Leads to Membrane Destabilization and Foliar Injury in Red Spruce. *BioScience* 49 (10): 789–800 https://doi.org/10.2307/1313570.

Driscoll, C.T. et al. 2001. Acidic Deposition in the Northeastern United States: Sources and Inputs, Ecosystem Effects, and Management Strategies. *BioScience* 51 (3): 180–98. https://doi.org/10.1641/0006-3568(2001)051[0180:ADITNU]2.0.CO;2.

Engel, B.J. et al. 2016. Assessing Relationships Between Red Spruce Radial Growth and Pollution Critical Load Exceedance Values. *Forest Ecology and Management* 359: 83–91. https://doi.org/10.1016/j.foreco.2015.09.029.

Fernandez, R., and Zegre, N. 2019. Seasonal Changes in Water and Energy Balances over the Appalachian Region and Beyond Throughout the Twenty-First Century. *Journal of Applied Meteorology and Climatology* 58 (5): 1079–1102. https://doi.org/10.1175/JAMC-D-18-0093.1.

Fraver, S., White, A.S., and Seymour, R.S. 2009. Natural Disturbance in an Old-Growth Landscape of Northern Maine, USA. *Journal of Ecology* 97 (2): 289–98. https://doi.org/10.1111/j.1365-2745.2008.01474.x.

George, S.S. 2014. An Overview of Tree-Ring Width Records across the Northern Hemisphere. *Quaternary Science Reviews* 95: 132–50. https://doi.org/10.1016/j.quascirev.2014.04.029.

Greaver, T.L. et al. 2012. Ecological Effects of Nitrogen and Sulfur Air Pollution in the US: What Do We Know? *Frontiers in Ecology and the Environment* 10 (7): 365–72. https://doi.org/10.1890/110049.

Harley, G.L. et al. 2021. Towards Broad-Scale Temperature Reconstructions for Eastern North America Using Blue Light Intensity from Tree Rings. *International Journal of Climatology* 41 (S1): E3142–59. https://doi.org/10.1002/joc.6910.

Heeter, K.J., Harley, G.L., Van De Gevel, S.L., and White, P.B. 2019. Blue Intensity as a Temperature Proxy in the Eastern United States: A Pilot Study from a Southern Disjunct Population of *Picea rubens* (Sarg.). *Dendrochronologia* 55: 105–9. https://doi.org/10.1016/j.dendro.2019.04.010.

Holmes, R.L. 1983. Computer-Assisted Quality Control in Tree-Ring Dating and Measurement. *Tree-Ring Bulletin* 43: 69–78. https://repository.arizona.edu/handle/10150/261223.

Johnson, A.H., Cook, E.R., and Siccama, T.G. 1988. Climate and Red Spruce Growth and Decline in the Northern Appalachians. *Proceedings of the National Academy of Sciences* 85 (15): 5369–73. https://doi.org/10.1073/pnas.85.15.5369.

Keppel, G. et al. 2012. Refugia: Identifying and Understanding Safe Havens for Biodiversity Under Climate Change. *Global Ecology and Biogeography* 21(4): 393-404. https://doi.org/10.1111/j.1466-8238.2011.00686.x.

Koo, K.A., Patten, B.C., and Teskey, R.O. 2011. Assessing Environmental Factors in Red Spruce (*Picea rubens* Sarg.) Growth in the Great Smoky Mountains National Park, USA: From Conceptual Model, Envirogram, to Simulation Model. *Ecological Modeling* 222 (3): 824–34. https://doi.org/10.1016/j.ecolmodel.2010.11.020.

Kosiba, A.M., Schaberg, P.G., Hawley, G.J., and Hansen, C.F. 2013. Quantifying the Legacy of Foliar Winter Injury on Woody Aboveground Carbon Sequestration of Red Spruce Trees. *Forest Ecology and Management 302*: 363–71. https://doi.org/10.1016/j.foreco.2013.03.006.

Kosiba, A.M., Schaberg, P.G., Rayback, S.A., and Hawley, G.J. 2017. Comparative Growth Trends of Five Northern Hardwood and Montane Tree Species Reveal Divergent Trajectories and Response to Climate. *Canadian Journal of Forest Research* 47 (6): 743–54. https://doi.org/10.1139/cjfr-2016-0308.

Kosiba, A.M., Schaberg, P.G., Rayback, S.A., and Hawley, G.J. 2018. The Surprising Recovery of Red Spruce Growth Shows Links to Decreased Acid Deposition and Elevated Temperature. *Science of the Total Environment* 637: 1480–91. https://doi.org/10.1016/j.scitotenv.2018.05.010.

Larsson 2014 CooRecorder And Cdendro Programs of the CooRecorder/Cdendropackage. Version 7.7. Retrieved from http://www.cybis.se/forfun/dendro/.

Mathias, J.M., and Thomas, R.B. 2018. Disentangling the Effects of Acidic Air Pollution, Atmospheric CO_2, and Climate Change on Recent Growth of Red Spruce Trees in the Central Appalachian Mountains. *Global Change Biology* 24 (9): 3938–53. https://doi.org/10.1111/gcb.14273.

McLaughlin, S.B., Downing, D.J., T. J. Blasing, E. R. Cook, and Adams, H.S. 1987. An Analysis of Climate and Competition as Contributors to Decline of Red Spruce in High Elevation Appalachian Forests of the Eastern United States. *Oecologia* 72: 487–501. https://doi.org/10.1007/BF00378973.

Mello, R.A. 1987. *Last Stand of the Red Spruce*. Washington, DC: Island Press.

Mosteller, F., and Tukey, J.W. 1977. Data Analysis and Regression: A Second Course in Statistics. Reading: Addison-Wesley Series in Behavioral Science, Quantitative Methods.

Nicault, A. et al. 2015. Spatial Analysis of Black Spruce (*Picea mariana* (Mill.) BSP) Radial Growth Response to Climate in Northern Québec–Labrador Peninsula, Canada. *Canadian Journal of Forest Research* 45 (3): 343–52. https://doi.org/10.1139/cjfr-2014-0080.

Perry, L.B., and Konrad, C.E. 2006. Relationships Between NW Flow Snowfall and Topography in the Southern Appalachians, USA. *Climate Research* 32 (1): 35–47. https://doi:10.3354/cr032035.

Prat, O.P., and Barros, A.P. 2010. Ground Observations to Characterize the Spatial Gradients and Vertical Structure of Orographic Precipitation–Experiments in the Inner Region of the Great Smoky Mountains. *Journal of Hydrology* 391 (1-2): 141–56. https://doi.org/10.1016/j.jhydrol.2010.07.013.

PRISM. 2022. PRISM Climate Group, Oregon State University. http://www.prism.oregonstate.edu/. Accessed on February 14, 2022.

Rodionov, S. N. 2004. A Sequential Algorithm for Testing Climate Regime Shifts. *Geophysical Research Letters* 31 (9): L09204. https://doi.org/10.1029/2004GL019448.

Schaberg, P.G. et al. 2000. Acid Mist and Soil Ca and Al Alter the Mineral Nutrition and Physiology of Red Spruce. *Tree Physiology* 20 (2): 73–85. https://doi.org/10.1093/treephys/20.2.73.

Schuler, T.M., and Collins, R.J. 2002. Successional Dynamics and Restoration Implications of a Montane Coniferous Forest in the Central Appalachians, USA. *Natural Areas Journal* 22 (2): 88–98.

Soulé, P.T. 2011. Changing Climate, Atmospheric Composition, and Radial Tree Growth in a Spruce-Fir Ecosystem on Grandfather Mountain, North Carolina. *Natural Areas Journal* 31 (1): 65–74. http://dx.doi.org/10.3375/043.031.0108.

Southern Appalachian Spruce Restoration Initiative. 2022. https://southernspruce.org/. Accessed on June 13, 2022.

Speer, J.H., Grissino-Mayer, H.D., Orvis, K.H., and Greenberg, C.H. 2009. Climate Response of Five Oak Species in the Eastern Deciduous Forest of the Southern Appalachian Mountains, USA. *Canadian Journal of Forest Research* 39 (3): 507–18. https://doi.org/10.1139/X08-194.

Stahle, D.W., Fye, F.K., Cook, E.R., and Griffin, R.D. 2007. Tree-Ring Reconstructed Megadroughts Over North America Since AD 1300. *Climatic Change* 83 (1): 133–49. https://doi.org/10.1007/s10584-006-9171-x.

United States Forest Service. 2022. The Spruce-Fir Ecosystem. Retrieved from https://www.fs.usda.gov/Internet/FSE_DOCUMENTS/stelprdb5436769.pdf.

Wason, J.W., and Dovciak, M. 2017. Tree Demography Suggests Multiple Directions and Drivers for Species Range Shifts in Mountains of Northeastern United States. *Global Change Biology* 23 (8): 3335–47. https://doi.org/10.1111/gcb.13584.

White, P.B. 2010. Decadal-scale trends in forest succession and climatic sensitivity in a red spruce-Fraser fir forest at Roan Mountain, Pisgah and Cherokee national forests. Masters thesis. Appalachian State University, Boone.

White, P.B., Soulé, P., and van de Gevel, S. 2014. Impacts of Human Disturbance on the Temporal Stability of Climate–Growth Relationships in a Red Spruce Forest, Southern Appalachian Mountains, USA. *Dendrochronologia* 32 (1):71–77. https://doi.org/10.1016/j.dendro.2013.10.001.

White, P.S., and Cogbill, C.V. 1992. Spruce-Fir Forests of Eastern North America. In *Ecology and Decline of Red Spruce in the Eastern United States,* edited by C. Eager and M. Adams. 3–39. Springer.

Wigley T.M., Briffa, K.R. and Jones, P.D. 1984. On the Average Value of Correlated Time Series, with Applications in Dendroclimatology and Hydrometeorology. *Journal of Climate and Applied Meteorology* 23 (2): 201–13. https://doi.org/10.1175/1520-0450(1984)023<0201:OTAVOC>2.0.CO;2.

Yetter, E., Chhin, S., and Brown, J.P. 2021. Sustainable Management of Central Appalachian Red Spruce. *Sustainability* 13 (19): 10871. https://doi.org/10.3390/su131910871.

Zang, C., and Biondi, F. 2015 Treeclim: an R Package for the Numerical Calibration of Proxy-Climate Relationships. *Ecography* 38 (4): 431–36. https://doi.org/10.1111/ecog.01335.

Zhang, Y., Bergeron, Y., Zhao, X.H., and Drobyshev, I. 2015. Stand History Is More Important than Climate in Controlling Red Maple (*Acer rubrum* L.) Growth at its Northern Distribution Limit in Western Quebec, Canada. *Journal of Plant Ecology* 8 (4): 368–79. https://doi.org/10.1093/jpe/rtu029.

DR. MAEGEN ROCHNER (maegen.rochner@louisville.edu, @MRochner86) is an Assistant Professor in the Department of Geographic and Environmental Sciences at the University of Louisville in Louisville, Kentucky, 40292. Her research interests include all applications of dendrochronology, but her current focus is on dendroarchaeology and urban dendrochronology in the southeastern United States.

DR. TOMMY PATTERSON (tpatt@ad.unc.edu) is a STEM Learning Specialist and Coach in the Learning Center at the University of North Carolina in Chapel Hill, North Carolina, 27599. His research interests include dendroecology and climatology with a focus on longleaf pine ecosystems.

DR. KAREN HEETER (kheeter@ldeo.columbia.edu, @dendrokurnology) is a Postdoctoral Research Fellow at Columbia University's Lamont-Doherty Earth Observatory in Palisades, New York, 10964. Her research interests include paleoclimatology and biogeography.

DR. GRANT L. HARLEY (gharley@uidaho.edu, @dendrotrog) is an Associate Professor of Geography in the Department of Earth and Spatial Sciences at the University of Idaho in Moscow, Idaho, 83844. His research interests include Quaternary landscape dynamics and paleoenvironmental reconstruction.